

Fabrication of poly(ϵ -caprolactone)-embedded lignin-chitosan nanocomposite porous scaffolds from Pickering emulsions

Yaozong Li,^a Yingying Peng,^a Yang Hu,^{a,*} Jian Liu,^a Teng Yuan,^a Wuyi Zhou,^a
Xianming Dong,^a Chaoyang Wang,^b Bernard P. Binks,^{c,*} Zhuohong Yang^{a, d,*}

^a *Key Laboratory for Biobased Materials and Energy of Ministry of Education,
College of Materials and Energy, South China Agricultural University,
Guangzhou 510642, China*

^b *Research Institute of Materials Science, South China University of Technology,
Guangzhou 510640, China*

^c *Department of Chemistry, University of Hull, Hull. HU6 7RX. UK*

^d *Maoming Branch, Guangdong Laboratory for Lingnan Modern Agriculture,
Maoming 525000, China*

* Corresponding authors

huyang0303@scau.edu.cn; b.p.binks@hull.ac.uk; yangzhuohong@scau.edu.cn

Revision submitted to Langmuir on 19.4.23

Contains Supporting Information

ABSTRACT

Poly(ϵ -caprolactone) (PCL)-incorporated lignin-chitosan biomass-based nanocomposite porous scaffolds have been effectively prepared by templating oil-in-water Pickering high internal phase emulsions (HIPEs). PCL is dissolved in oil and chitosan and lignin nanoparticles originate in water. The continuous phase of the emulsions is gelled by cross-linking of chitosan with genipin and then freeze dried to obtain porous scaffolds. The resulting scaffolds display interconnected and tunable pore structures. An increase in PCL content increases the mechanical strength and greatly reduces the water absorption capacity of the scaffolds. Scaffolds loaded with the anti-bacterial drug enrofloxacin show a slow drug release profile, adjustable release rate and favourable long-term anti-bacterial activity. Moreover, Pickering emulsion templates with suitable viscosity are used as 3D printing inks to construct porous scaffolds with personalized geometry. The results imply that the simplicity and versatility of the technique of combining freeze drying with Pickering HIPE templates is a promising approach to fabricate hydrophobic biopolymer-incorporated biomass-based nanocomposite porous scaffolds for biomedical applications.

Keywords: Pickering emulsion, lignin, chitosan, poly(ϵ -caprolactone), porous scaffold, 3D printing

INTRODUCTION

Porous scaffolds consisting of bio-based compositions with adjustable microstructures have attracted much attention in biomedical applications such as biosensing, bioseparation, biocatalysis, drug delivery and tissue engineering,¹⁻⁴ because of their large surface area, favourable biocompatibility, suitable biodegradability, low density and high porosity. Recently, various natural and synthetic degradable biopolymer materials have been used to develop bio-based porous scaffolds.⁵⁻⁷ Biorenewable polymers from natural resources are gaining increasing interest as the building blocks for environmentally benign bio-based porous scaffolds.⁸⁻¹⁰

Chitosan is a renewable cationic polysaccharide prepared by alkaline N-deacetylation of chitin,¹¹⁻¹² which is an abundant natural biopolymer and widely found in certain natural crustacean shells including crab and shrimp. Chitosan has been widely investigated for the construction of bio-based porous scaffolds for various applications including tissue engineering scaffolds,¹³ porous separation media^{14,15} and drug carriers,¹⁶ due to its favourable biocompatibility, antimicrobial and antioxidant activity, biodegradability, hydrophilic nature, adsorption and affinity capacity, reactivity and easy processability.^{17,18} Nevertheless, pure chitosan porous scaffolds are weak mechanically and suffer to maintain their structure in aqueous environments (especially in acid) because the highly hydrophilic nature of chitosan allows it to uptake water easily which restricts applications of the related porous scaffolds.^{19,20} To alleviate the above issues, a highly acceptable and efficient strategy is developed by combining

chitosan with other materials to enhance the mechanical stability and reduce the water absorption behaviour of the porous scaffolds.

Lignin is the second most abundant bio-renewable polymer after cellulose accounting for 20-30% of the cell walls of plants,^{21,22} and is beneficial to the mechanical strength and rigidity of vascular plants.²³⁻²⁵ Annually, 50-70 million tons of lignin is generated as a by-product in the preparation of wood pulp and lignocellulosic bioethanol.²⁶ However, lignin has generally been used in low value applications,²⁷⁻²⁹ such as bio-renewable fuel, fertilizer and adhesives. It is necessary to develop new avenues for the high value utilization of lignin in the preparation of sustainable materials, which have promising potential to resolve the problem of the fast depletion of fossil resources. Lignin possesses typical favourable characteristics of biocompatibility, antimicrobial activity, renewability, adsorption performance, antioxidant property and abundance.³⁰⁻³³ All these **propel** lignin as an interesting building block of scaffold biomaterials for biomedical applications. In view of its poor solubility and fragile nature, a strategy to improve the use of lignin in preparing porous scaffolds is to create a composite by combining lignin nanoparticles with other biopolymers. Interestingly, lignin nanoparticles have been successfully applied to reinforce phenolic foams,³⁴ polyacrylamide hydrogels³⁵ and chitosan-polyvinyl alcohol porous scaffolds.²⁰ Nevertheless, it is still a challenge for composite porous scaffolds of hydrophilic natural biopolymers (*e.g.* chitosan) and lignin nanoparticles to retain their mechanical stability in aqueous environments because of swelling. One of the effective approaches to overcome this is the incorporation of hydrophobic polymers

into the scaffold. Among various hydrophobic polymers, poly(ϵ -caprolactone), PCL, has been widely utilized to prepare porous scaffolds for biomedical applications, because of its favourable mechanical property, easy processability, good biocompatibility and adjustable biodegradability.³⁶⁻³⁸ Abudula and coworkers fabricated PCL-coated chitin-lignin porous scaffolds with core-shell fibers by coaxial electrospinning.³⁹ However, the electrospinning method was a relatively time-consuming approach for large scale production and it was difficult to adjust the pore structure and geometry of the porous scaffolds. Hence, it is desirable to develop a facile and effective approach for the construction of PCL-incorporated lignin-hydrophilic natural biopolymer nanocomposite porous scaffolds with tunable porous structure and required shape.

Pickering high internal phase emulsions (HIPEs) are stabilized by solid particles with the internal phase volume being more than 74%,^{40,41} and have been regarded as an effective template to construct porous scaffolds.⁴² The pore structure of the porous scaffold prepared using Pickering HIPEs can be easily regulated by adjusting the emulsion composition. In our previous work, we successfully constructed inorganic nanoparticle-stabilized water-in-oil Pickering HIPEs and used them as templates to prepare inorganic nanoparticle/polyester porous scaffolds.^{37,43} The prepared Pickering HIPEs displayed high viscosity and shear thinning behavior, which endowed them with 3D printability to construct porous scaffolds with personalized shape and structure. However, the inorganic nanoparticles had to be hydrophobically modified before emulsion preparation, which hinders large scale preparation of scaffolds. Thus, the

direct application of Pickering HIPE stabilizers without *ex situ* modification is desirable for the facile and large scale preparation of Pickering HIPEs template-based porous scaffolds.

In this study, we develop an effective and one-pot method to prepare PCL-incorporated lignin-chitosan nanocomposite porous scaffolds with adjustable microstructure based on templating oil-in-water (O/W) Pickering HIPEs. Specifically, O/W Pickering HIPEs were directly prepared by emulsification of an aqueous phase containing lignin nanoparticles, chitosan and genipin with an oil phase solution of PCL in dichloromethane. The lignin nanoparticles and chitosan act as the co-stabilizers of emulsion droplets and were used directly to prepare stable HIPEs without prior modification. Subsequently, emulsion hydrogels were formed by *in situ* gelation of the continuous water phase triggered *via* the crosslinking of chitosan with genipin. Moreover, the PCL-embedded lignin-chitosan porous scaffolds were obtained after removing both solvents by freeze-drying of the emulsion hydrogels. A schematic diagram of the scaffold preparation is shown in Figure 1. The droplet morphology and rheological behavior of Pickering HIPEs were investigated. Furthermore, the porous structure, mechanical performance, water absorption behavior, enrofloxacin loading and release property and antibacterial activity of the porous scaffolds were evaluated in detail. In addition, the 3D printability of Pickering HIPEs was investigated for constructing porous scaffolds with designed structures and personalized geometry.

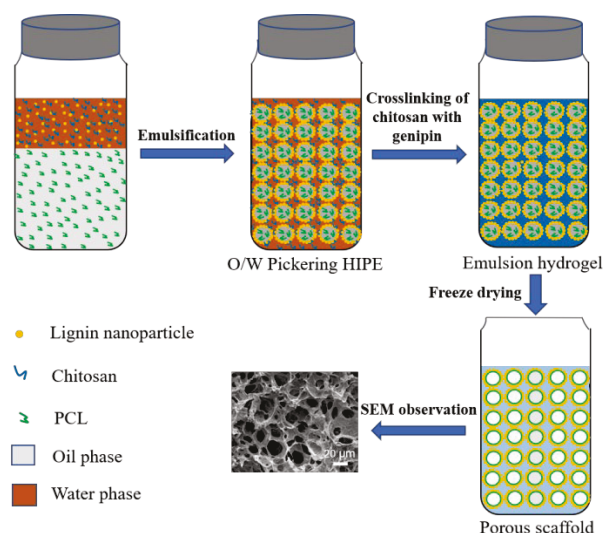


Figure 1. Schematic illustration of the formation of PCL-embedded lignin-chitosan nanocomposite porous scaffolds from O/W Pickering HIPE templates.

EXPERIMENTAL

Materials

Chitosan (deacetylation degree 95.3% and weight-average molecular weight 300,000 g/mol) was purchased from Shandong Haili Medical Instrument (China) and its chemical structure is shown in Figure S1a. PCL (weight-average molecular weight 50,000 g/mol) was provided by BASF (Germany). Lignin was provided by Meadwestvaco Corporation (USA). Dichloromethane was obtained from Guangzhou Chemical Factory (China). Genipin was purchased from Baoji Rundekang Biotechnology Co. Ltd. (China) and its chemical structure is shown in Figure S1b. **Acridine orange was purchased from Nanjing duly Biotechnology Co. Ltd. (China).** Phosphate buffer saline (PBS) was obtained from Shanghai Double Helix Biotechnology Co. Ltd. (China). Enrofloxacin (ENR) was purchased from Aladdin (China). Sodium hydroxide and concentrated hydrochloric acid were bought from

Guangzhou Chemical Factory (China). In this study, the used water (resistivity > 18.0 M Ω cm) was purified using a Millipore direct-Q-3 purification instrument (USA).

Methods

Preparation of lignin nanoparticles and Pickering HIPEs

The lignin nanoparticles were fabricated by regulating the pH value of aqueous lignin solutions. Firstly, lignin was purified by the method of alkali-solution and acid-isolation,⁴⁴ and the detailed purification steps are described in the Supporting Information. Afterwards, 1.2 g of the purified lignin powder was added into a vial containing 26 mL water and then stirred for 30 min in an ice bath. After that, 1 M NaOH solution was slowly added to raise the pH value to around 11 and fully dissolve lignin. Subsequently, 1 M HCl solution was added dropwise into the lignin solution until the pH value reached 3 to obtain a 4 w/v% lignin nanoparticle suspension.

The formation of O/W HIPEs ($\phi_0 = 0.75$) was carried out as follows. Firstly, three solutions were prepared with magnetic stirring. 8 w/v% chitosan solution was prepared by dissolving chitosan in 1 v/v% glacial acetic acid. 2 w/v% genipin solution was prepared by dissolving genipin in water. PCL solution was formed by dissolving it in dichloromethane. Thereafter 2 mL lignin nanoparticle suspension, 2 mL chitosan solution, 50 μ L genipin solution were added respectively into a glass vial and mixed well under ultrasound treatment for 30 min in an ice-water bath to obtain the aqueous phase. Moreover, 12 mL PCL solution was added into the aqueous phase in batches and emulsified at 3,500 rpm for 12 min a Haimen Kylin-Bell QL-866 vorter mixer (China) to obtain Pickering HIPEs. Various concentrations of PCL (2, 4, 8, 12 w/v%) were used

to prepare HIPES. As a control, an emulsion without PCL in the oil phase was also prepared.

Preparation of nanocomposite porous scaffolds

In this study, nanocomposite porous scaffolds were constructed from Pickering emulsion templates. The obtained Pickering HIPES prepared above were held at room temperature for 24 h to gel the aqueous phase. Subsequently, the obtained emulsion hydrogels were placed in a freezer at -18 °C for 24 h. The porous scaffolds were obtained after being freeze dried at -45 °C in a Boyikang FD-1A-50 freeze dryer (China) for 24 h.

Porosity determination

The mass and volume of porous scaffolds were accurately determined with a gravimetric balance and a digital caliper, respectively. Subsequently, the porous scaffold samples were compressed and densified using a Shimadzu SSP-10A tablet press machine and the volume of the fully dense scaffold was measured using a digital caliper. The bulk density of the composite porous scaffold (ρ_a) and the density of the fully dense scaffold (ρ_b) were calculated by dividing their mass by their volume, respectively. Three individual tests for each formulation were performed to attain the mean value. The porosity of a porous scaffold (Φ) was calculated using

$$\Phi (\%) = (1 - \rho_a / \rho_b) \times 100 \quad (1)$$

Mechanical property measurement

The mechanical properties in compression of composite porous scaffolds were determined using a Shimadzu AGS-X universal testing machine equipped with a 1 KN

load cell at room temperature. The cylindrical scaffold samples of diameter 10 mm and height 15 mm were used for the compression test. The measurement was performed at a compression speed of 2 mm min⁻¹. Moreover, the stress-strain curves of the test scaffold samples were recorded. At least three samples are used to characterize the compressive properties of the composite porous scaffold for each formulation.

Water absorption behavior study

The water absorption behavior of the composite porous scaffolds was performed in water at 25 °C. Dried porous scaffolds were weighed and denoted as W_d and then incubated at 25 °C in water. At pre-determined time intervals, the swollen scaffold sample was taken out, thoroughly wiped with filter paper and weighed (W_s). All measurements were repeated five times. The water absorption percentage (WAP) of composite scaffold was calculated using

$$\text{WAP (\%)} = (W_s - W_d) / W_d \times 100 \quad (2)$$

in vitro drug release

ENR was used as a model drug to study the drug release performance of the composite porous scaffolds. The preparation protocol of drug-loaded scaffolds was the same as that of composite porous scaffolds described above except that ENR (4 wt.% with respect to the mass of polymers and nanoparticles) was dissolved in oil before emulsification. The *in vitro* drug release study was performed as follows. Firstly, the pre-weighed drug-loaded scaffold (approximately 25 mg) was placed into an erlenmeyer flask containing 50 mL of PBS solution (pH = 7.4). The flask was incubated in a 37 °C water bath under a constant vibration speed of 120 rpm. At a pre-determined

time interval, 2 mL of the release medium was taken out and was quantitatively measured at the maximum absorption wavelength of 271 nm *via* a Techcomp UV2300 ultraviolet spectrophotometer. After that, the tested release medium was poured back into the erlenmeyer flask. The release percentage of ENR from the drug-loaded scaffold was calculated based on the standard absorbance-concentration curve established with known concentrations of ENR in PBS. Three samples were used for each scaffold to obtain the average value.

Antibacterial activity testing

Escherichia coli (*E. coli*) and *Staphylococcus aureus* (*S. aureus*) were employed to investigate the antibacterial activity of the composite porous scaffolds according to our previous work⁴³ with a minor modification. Herein, the antibacterial activities of the composite porous scaffolds with and without ENR were studied by evaluating the inhibition zone against *E. coli* and *S. aureus*. Firstly, the ENR-loaded scaffolds and the blank scaffolds without ENR were cut into circular sheets of diameter 6 mm and thickness 1 mm. Sterilized agar medium was poured into glass culture dishes and then completely gelled to form nutrient agar plates. 1 mL of the bacterial suspension (10^5 cells/mL) was taken and evenly coated onto the nutrient agar plate. The scaffold sample was placed onto the surface of the plate which was incubated at 37 °C for 7 days. At a pre-determined time interval, nutrient agar plates were photographed using a digital camera.

Characterization

The **morphologies** of lignin nanoparticles and **complex nanoparticles (chitosan-**

adsorbed lignin nanoparticles) were observed using a FEI Tecnai type 12 transmission electron microscope (TEM) by applying an acceleration voltage of 200 kV. Before observation, the diluted suspension of lignin nanoparticles and complex nanoparticles were respectively dropped on copper meshes and they were imaged after drying. Herein, for the formation of the complex nanoparticles, 2 mL lignin nanoparticle suspension (4 w/v%) was thoroughly mixed with 2 mL chitosan solution (8 w/v%) under ultrasound treatment for 30 min, and the electrostatic interaction between positively charged chitosan molecules and negatively charged lignin nanoparticles resulted in the formation of chitosan-adsorbed lignin nanoparticles. The particle size distributions of lignin nanoparticles and complex nanoparticles were measured with a Nano ZSE-type Malvern Zetasizer analyzer, and zeta potentials of lignin nanoparticles and complex nanoparticles were also determined with the same instrument based on measuring the electrophoretic mobility and then applying the Henry equation. The Pickering HIPEs were observed using a Phenix BMC500 optical microscope. Confocal laser scanning microscopy (CLSM) was performed with a Leica TCS SP8 STED 3X instrument. The lignin nanoparticles were visualized after labelling with acridine orange at an excitation wavelength of 488 nm. The viscosity of Pickering HIPEs was measured using an Anton Paar MCR502 rheometer equipped with stainless steel parallel plate geometry (40 mm in diameter) at 25 °C in the shear rate range from 0.01 to 10 s⁻¹. The microstructure of the scaffold cross-sections was observed using a Zeiss EVO 18 scanning electron microscope (SEM) at an accelerating voltage of 10 kV. For SEM observation, the specimens were cryo-fractured by immersion in liquid nitrogen and then sputter coated

with a thin gold layer. The droplet sizes of Pickering HIPEs and the resulting pore sizes of porous scaffolds were measured and analyzed by the Nano Measurer 1.2 software, and at least 40 droplets and pores were imaged to obtain their size distributions. Thermal gravimetric analysis (TGA) of the samples were performed using a Netzsch TG 209 F1 Libra analyzer. Fourier transform infrared (FTIR) spectra of the samples were acquired using a Bruker Vertex 70 spectrometer in the attenuated total reflection mode ranging from 4000 to 500 cm^{-1} .

3D printing of Pickering HIPEs

3D printing was carried out using a Xutong commercial desktop ADT-TV5300DJ three axis dispenser (China) fitted with a pneumatic pressure-driven extrusion polypropylene syringe. Briefly, the Pickering HIPE was added into the cartridge of the polypropylene syringe equipped with a conical needle (size 17 gauge with internal diameter of 1.10 mm). Afterwards, the syringe was fixed on the dispenser and connected to the three axis dispensing control system. The Pickering HIPE was extruded from the cartridge and promptly printed layer by layer on a glass panel at room temperature to build the designed emulsion scaffolds of cubic shape. For the best result, the linear printing speed was set to 30 mm s^{-1} , while the extrusion pressures in the range from 20 to 100 kPa were slightly adjusted for every HIPE during the printing process. After 3D printing, the sealed emulsion scaffolds were placed at room temperature for 24 h to gel and finally obtain the printed hydrogel scaffolds. Printed hydrogel scaffolds were held at $-18\text{ }^{\circ}\text{C}$ for 24 h and then freeze dried at $-45\text{ }^{\circ}\text{C}$ for 24 h to obtain the printed composite porous scaffolds.

RESULTS AND DISCUSSION

Fabrication of lignin nanoparticles and Pickering HIPEs

In this work, lignin nanoparticles were fabricated by reducing the pH value of aqueous lignin solutions to 3. The TEM image (Figure 2a and Figure S2a) shows that the obtained lignin nanoparticles were approximately spherical and their particle diameters were about 100-170 nm. The measured particle size distribution by light scattering (Figure 2b) of a dilute dispersion (0.01 wt.%) produced an average particle diameter of *ca.* 350 nm. This result indicates that the lignin nanoparticles are slightly flocculated in aqueous dispersion. In water (pH = 3.5), lignin nanoparticles possess negative charges on their surfaces (see Figure S2) while chitosan in solution displays positive charges on its molecules (isoelectric point around pH 6.8). Thus, positively charged chitosan molecules can be adsorbed onto negatively charged lignin nanoparticles by electrostatic interaction to obtain chitosan-adsorbed lignin nanoparticles (namely complex nanoparticles) in water, which display improved emulsification capacity compared with bare lignin nanoparticles.⁴⁵ Moreover, the TEM image in Figure S3a demonstrates that the complex nanoparticles were quasi-spherical in shape and the particle size distribution (Figure S3b) results in a smaller average diameter (285 nm) to that of lignin nanoparticles.

O/W Pickering HIPEs were successfully fabricated by emulsifying oil containing PCL with water containing lignin nanoparticles, chitosan and genipin. The drop test (shown in Figure S4) verified that they were of the O/W type. As control experiments,

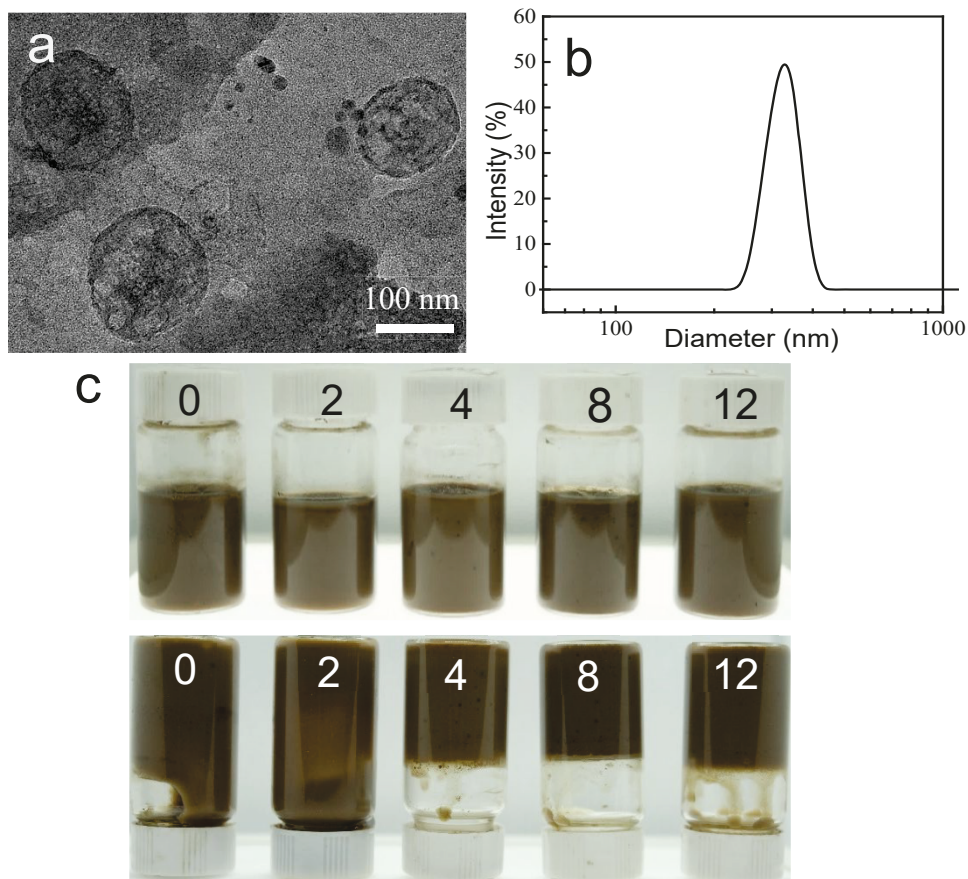


Figure 2. (a) TEM image of dry lignin nanoparticles and (b) size distribution of lignin nanoparticles in water. (c) Photos of fresh O/W Pickering HIPEs prepared with various PCL concentrations from 0 to 12 w/v% (upper - vessels upright, lower - vessels inverted).

the oil phase of PCL dichloromethane solution and aqueous phase including chitosan and genipin, oil phase of dichloromethane and aqueous phase of chitosan solution, oil phase of dichloromethane and aqueous phase of lignin nanoparticle suspension, oil phase of PCL dichloromethane solution and aqueous phase of lignin nanoparticle suspension, oil phase of PCL dichloromethane solution and aqueous phase including lignin nanoparticles and chitosan, oil phase of PCL dichloromethane solution and aqueous phase including lignin nanoparticles, chitosan and genipin, oil phase of dichloromethane and aqueous phase including lignin nanoparticles and chitosan were

all emulsified separately. As observed in Figure S5, the first four systems did not form stable HIPEs while the last three systems led to stable HIPEs without phase separation. The last three systems all contained lignin nanoparticles and chitosan in their water phases. The above result confirms that both chitosan and lignin nanoparticles present in the water phase were necessary to form stable Pickering HIPEs. It is noted that in water the negatively charged lignin nanoparticles could adsorb positively charged chitosan molecules onto their surfaces to form chitosan-adsorbed lignin nanoparticles (namely complex nanoparticles). Thus, it is concluded that complex nanoparticles were an effective particle emulsifier for stable emulsion formation. To verify the location of particle emulsifier at the oil-water interface, lignin nanoparticles were fluorescently labeled using acridine orange and then used to prepare a Pickering HIPE. The obtained CLSM image shown in Figure S6 shows bright green rings around the droplet interfaces indicating that the particle emulsifier is present to stabilize the emulsion. This is consistent with results reported in the literature^{46,47}. In addition, Figure 2c presents photos of Pickering HIPEs prepared with various PCL concentrations from 0 to 12 w/v%. The brown colour originates from lignin. We observed that the prepared Pickering HIPEs were viscous and increasing the PCL concentration in oil resulted in an increase in viscosity. When the PCL concentration ≥ 4 w/v%, the obtained HIPEs were gel-like and did not flow when the vessels were inverted.

The morphology of the fabricated HIPEs was observed by microscopy. Figure 3a-e displays the images for different PCL concentrations in the oil phase. The droplets were spherical and polydisperse in size. As seen from Figure S7, upon increasing the PCL concentration the average droplet diameter of HIPEs gradually increased. Since the viscosity of the oil phase increases with PCL concentration, this hindered the breakup of oil into droplets. Moreover, rheology measurements of the fabricated HIPEs

(Figure 3f) showed that they all possessed pronounced shear-thinning behavior. It was also seen that at low shear rate (0.01 s^{-1}), the HIPE with the highest PCL concentration had the highest viscosity producing gel-like HIPEs. After storing for 1 month at room temperature, HIPEs containing $\geq 4 \text{ w/v\%}$ PCL in oil displayed no coalescence or creaming (see Figure S8).

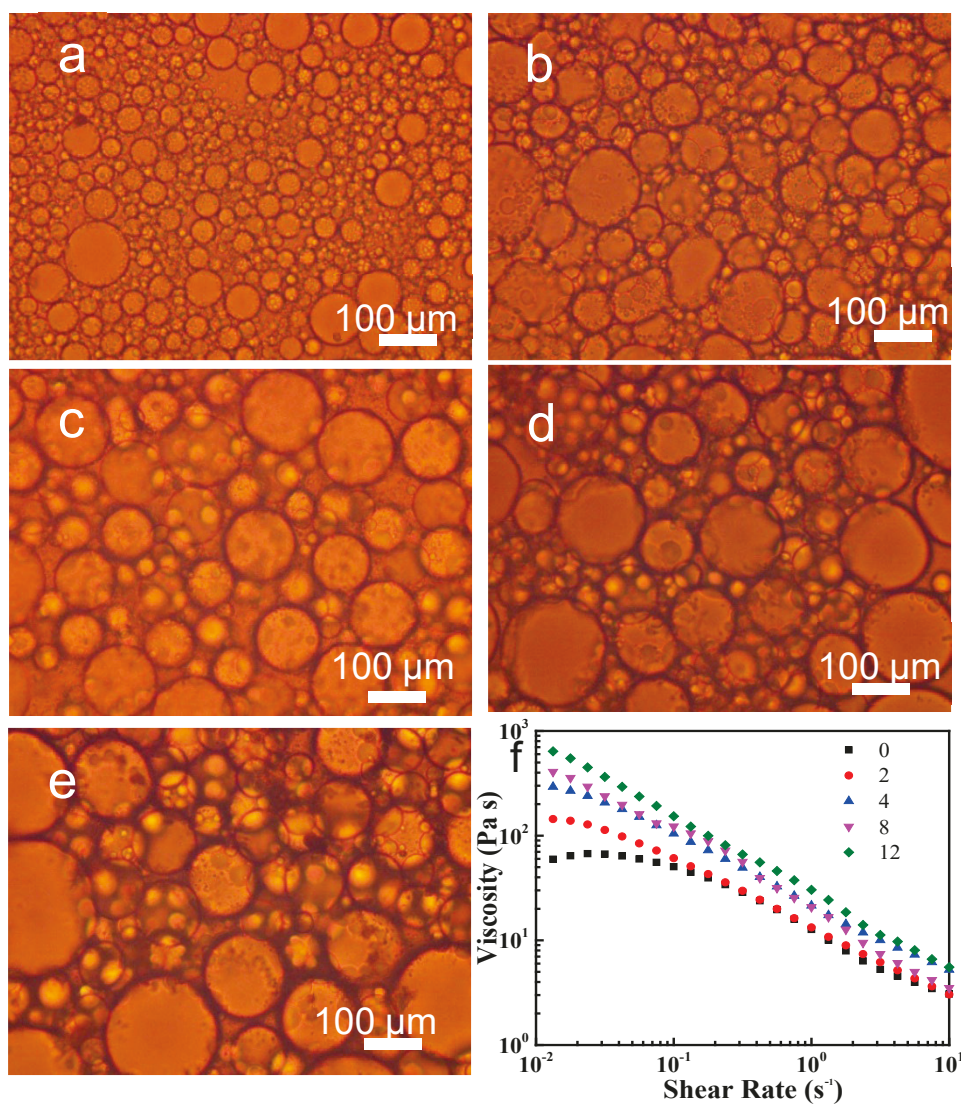


Figure 3. Optical micrographs of fresh O/W Pickering HIPEs with different PCL concentrations (w/v%): (a) 0, (b) 2, (c) 4, (d) 8, (e) 12. (f) Viscosity as a function of shear rate for emulsions in (a-e).

Fabrication and morphology of nanocomposite porous scaffolds

The nanocomposite porous scaffolds were obtained by first gelling the continuous water phase of HIPEs with subsequent freeze-drying. Gelation of the aqueous phase was realized *via* the cross-linking of chitosan induced by genipin as the cross-linking agent to obtain composite emulsion gels (see Figure S9). It was observed from Figure S9 that the newly prepared Pickering HIPE was brown in colour while that of the emulsion gel was blue. This phenomenon of blue colour formation was ascribed to the cross-linking reaction of chitosan and genipin, consistent with results in the previous literature.^{48,49} It is worth mentioning that genipin is a naturally occurring non-toxic cross-linker containing a dihydropyran ring and an ester group, and has attracted increasing interest because of its ability to cross-link chitosan containing primary amine groups. According to previous reports,^{50,51} the proposed reaction mechanism between genipin and chitosan under acidic conditions involves two reactions. The faster reaction is a nucleophilic attack from a primary amine group of chitosan on the C3 carbon atom of genipin to form a heterocyclic compound of genipin linked to the glucosamine residue in chitosan. The slower reaction is the nucleophilic substitution of the ester group from genipin to form a secondary amide linked to chitosan. Through the above two reactions, two molecules of chitosan can be cross-linked by one molecule of genipin (see Figure S10). Subsequently, the obtained emulsion gels were frozen in a refrigerator and then fully freeze dried to form composite porous scaffolds. The cross-section of the porous scaffolds was observed using SEM after spraying with gold in order to observe the inner pore structure.

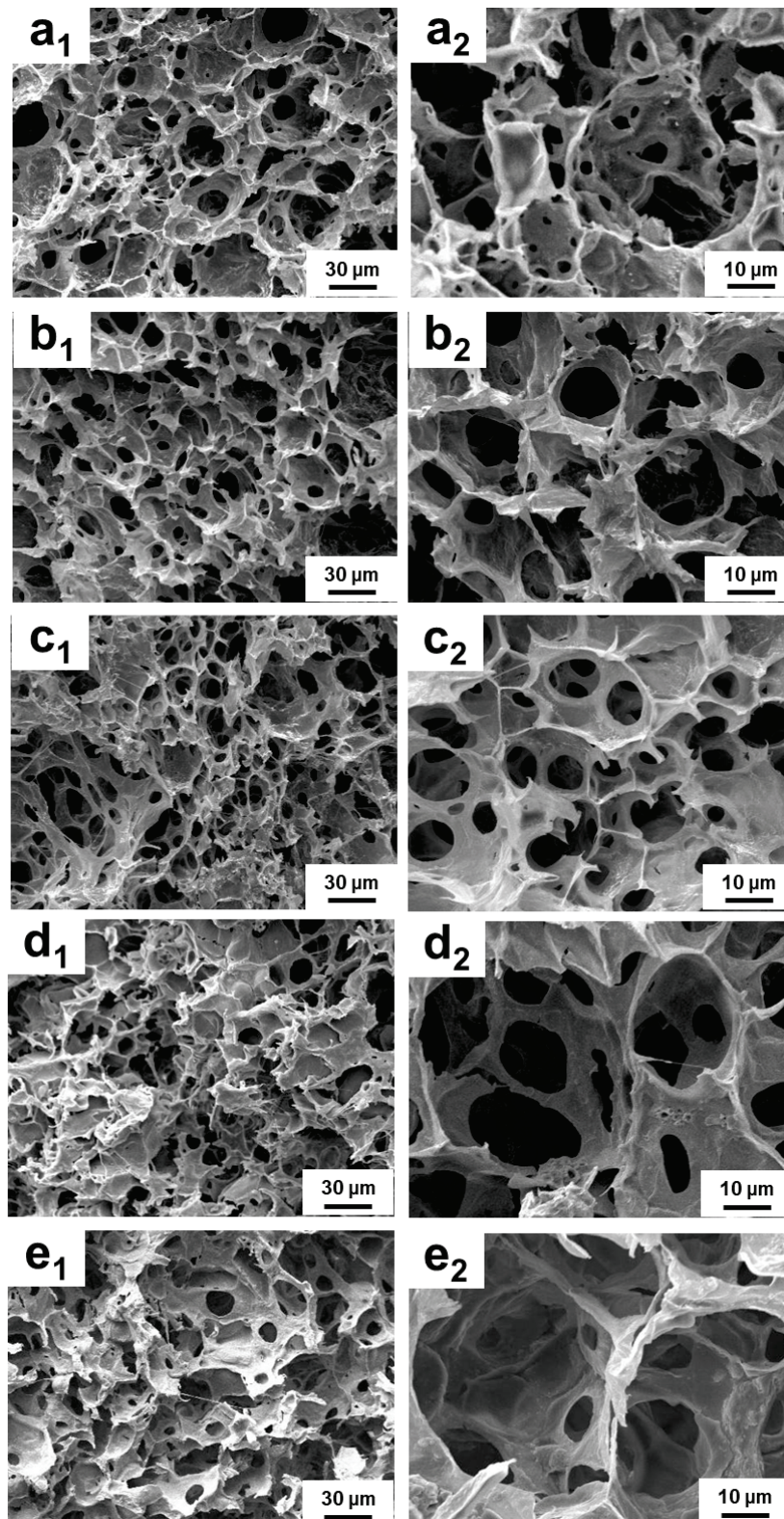


Figure 4. SEM micrographs at different magnifications of porous scaffolds prepared with different PCL concentrations (w/v%): (a) 0, (b) 2, (c) 4, (d) 8 and (e) 12.

Figure 4 contains SEM images of the porous scaffold prepared at different PCL concentrations. It could be seen that the composite porous scaffolds have a connected internal structure with pore sizes in the tens of microns. Moreover, compared with the average droplet diameter of HIPEs, the average pore diameter of composite porous scaffolds (Figure S11) was clearly smaller, which might be due to volume shrinkage caused by the high capillary force during drying. In addition, it was observed that the inner pore structure of the scaffolds prepared with PCL in oil had a visible difference compared with the control scaffold containing no PCL. The former possessed a PCL layer in the inner pore walls. Upon increasing the PCL concentration, the thickness of the polymer layer increases. The increase of PCL polymer layer thickness assisted in increasing the thickness and integrity of the scaffold pore walls. Table S1 lists the porosity of the composite porous scaffolds, which shows that it falls slightly with increasing PCL content. The very high porosity (> 93%) results in lightweight scaffolds which can be supported easily by the leaves of *setaria viridis* or other small green plants (Figure S12).

Mechanical property of porous scaffolds

The mechanical properties of porous scaffolds are vital to satisfy the application requirements. That is, the composite porous scaffolds should possess certain mechanical strength to support the three-dimensional shape and structure and to maintain the structural integrity during use. Compression tests were carried out to assess the mechanical property of the prepared scaffolds with varying PCL concentrations. Representative compressive stress-strain curves of the scaffolds are shown in Figure 5a.

It was observed that adding PCL had a significant impact on the compression property. The Young's modulus of porous scaffolds prepared with PCL concentration of 0, 2, 4, 8 and 12 w/v% were 0.14, 0.30, 0.75, 1.58 and 8.85 MPa respectively, and the related compression strengths (compressive stress at 75% strain) were 0.09, 0.16, 0.36, 0.75 and 4.18 MPa respectively. Upon increasing the PCL concentration to 8 w/v%, the compression strength and Young's modulus gradually increased. When the PCL concentration was increased to 12 w/v%, the compression strength and Young's

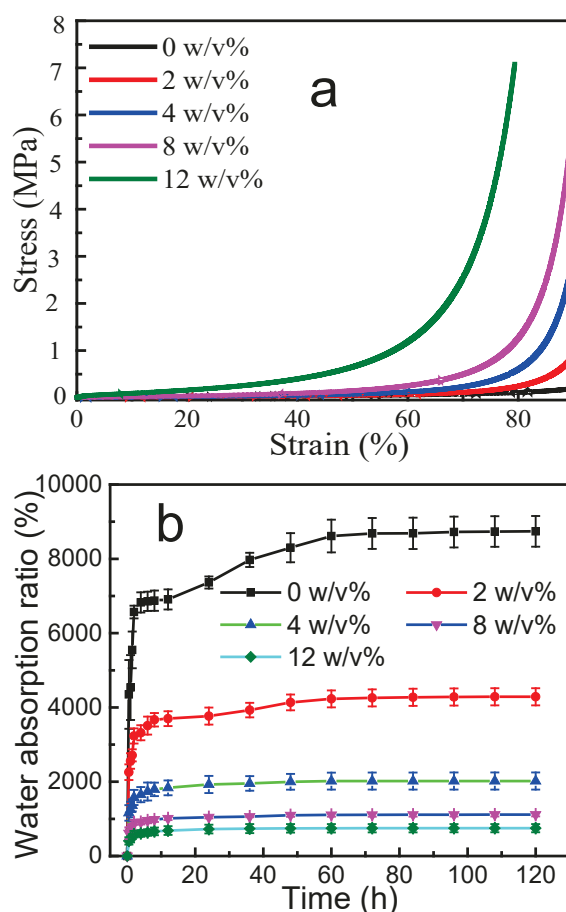


Figure 5. (a) Compressive stress-strain curves of composite porous scaffolds with different PCL concentrations containing genipin. (b) Water absorption ratio of composite porous scaffolds with different PCL concentrations after immersion in water as a function of time.

modulus improved markedly. The synthetic biodegradable polyester PCL possesses favorable mechanical properties alone. Augmenting the PCL concentration lowers the scaffold porosity increasing its density leading to an enhancement in the mechanical property of the scaffold. Composite scaffolds in the absence of cross-linking agent (Figure S13) displayed the lowest mechanical property compared with those containing genipin. The mechanical property of composite scaffolds is thus improved by adding PCL as well as cross-linking agent.

Water absorption and thermal behavior of porous scaffolds

When composite scaffolds containing hydrophilic materials are used in applications containing water, they tend to absorb water and swell. In this study, the water uptake behaviour of the composite scaffolds was investigated by measuring their weight increase after incubation in water. Figure 5b shows the time-dependent water absorption ratio of composite scaffolds with varying PCL content. As seen, the composite scaffold without PCL swelled fast by absorbing a mass of water in 1 h to reach a water absorption ratio of > 6000%. Its equilibrium water absorption ratio was nearly 9000% indicating that the chitosan-lignin composite scaffold had good water absorption ability. After decorating PCL in the inner pore walls, the water absorption rate of the composite scaffolds decreased significantly. The equilibrium water absorption ratios of scaffolds prepared with 2, 4, 8 and 12 w/v% PCL were around 4000%, 2000%, 1000% and 800%, respectively. As the concentration of PCL increased, the water absorption rate and extent of the composite scaffolds decreased. This is because PCL is a hydrophobic semi-crystalline polymer with limited water absorption capacity, and increasing the PCL content reduces the proportion of hydrophilic

substances. In addition, as the PCL concentration increased the porosity of the composite scaffolds decreased leading to a decrease in water absorption ability. Moreover, the thermal behavior of the porous scaffolds prepared with different PCL concentrations was examined using TGA (Figure S14). On increasing the PCL concentration, the mass loss curve shifted to higher temperature. The result is likely due to the densification of porous scaffolds at higher PCL content.

***in vitro* drug release study**

Drug release performance is an important index for the fabrication of porous composite scaffolds in biomedical applications. Herein, the potent anti-bacterial drug ENR is used as a model and loaded into composite scaffolds. ENR was added into the oil phase before HIPE preparation. FTIR measurements of composite scaffolds with or without ENR were made and the spectra are shown in Figure S15. In the presence of ENR, new peaks at 2829 and 1738 cm^{-1} appear originating from its characteristic peaks around 2866 and 1725 cm^{-1} . The release profiles of ENR-loaded composite scaffolds are shown in Figure 6. As seen, all the five drug-loaded composite scaffolds exhibited similar ENR release behavior, showing an initial burst release for the first 18 h and slower release subsequently. The initial fast release is attributed to the release of ENR from the outer surfaces and near the interior surfaces of the scaffold. The slow release is due to the decrease of ENR concentration difference between the composite scaffolds and the release medium. The release of ENR decreases as the PCL concentration increases due to both an increase in pore wall thickness by polymer and the reduced porosity.

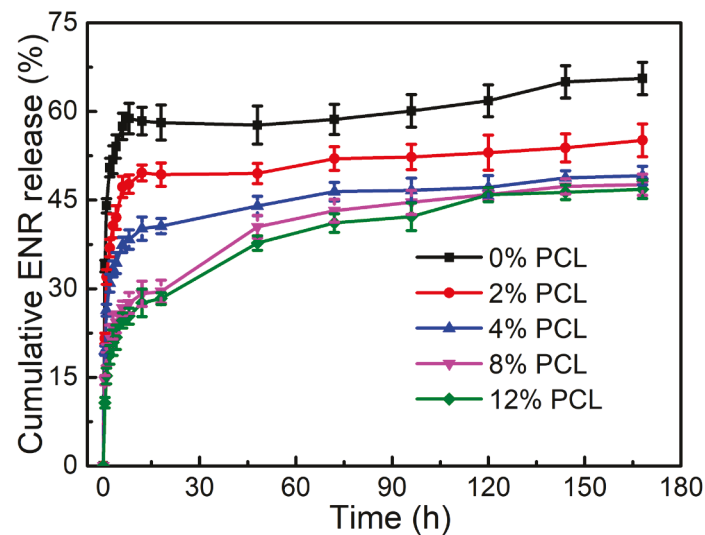


Figure 6. *in vitro* release profiles of ENR in PBS from ENR-loaded porous scaffolds prepared with different PCL concentrations.

Anti-bacterial activity

In this study, the composite scaffolds contained the anti-microbial polymer chitosan and lignin nanoparticles. Furthermore, ENR is a potent anti-bacterial drug and so it was also anticipated that ENR-loaded composite scaffolds would show improved anti-bacterial activity. The anti-bacterial activities of the ENR-loaded composite scaffolds prepared with a PCL concentration of 4 w/v% and the related composite scaffolds without ENR were assessed *via* the inhibition zone method using *E. coli* and *S. aureus* as the testing bacteria. Figure 7 shows the results of the above-mentioned composite porous scaffolds. The scaffold without ENR had clearly observable inhibition zones against both bacteria due to the presence of chitosan and lignin. After adding ENR, the inhibition zones were significantly greater confirming that ENR maintained its anti-bacterial activity after being loading into the scaffolds. We also noticed that the inhibition zones of the ENR-loaded composite scaffold showed no

observable reduction after 7 days incubation implying that they possessed a long-term and favourable anti-microbial effect.

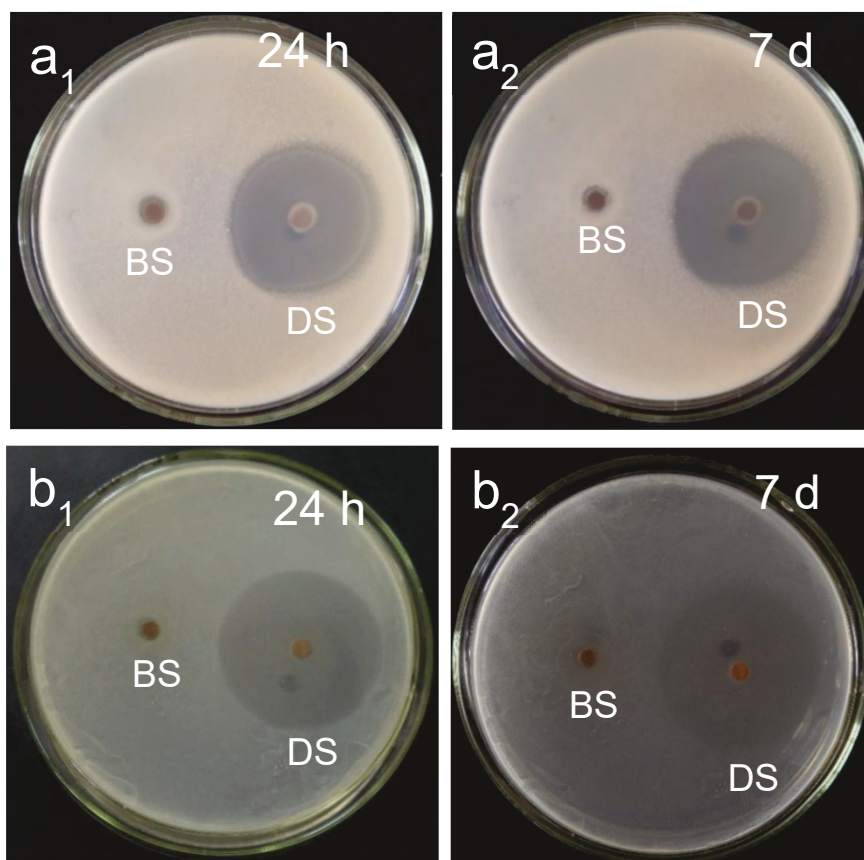


Figure 7. Anti-bacterial activity of the blank composite porous scaffold (BS) and the ENR-loaded composite porous scaffold (DS) prepared at a PCL concentration of 4 w/v% against (a) *S. aureus* and (b) *E. coli* with 24 h and 7 days incubation.

3D printing to construct scaffolds with specific geometry

The personalized fabrication of artificial porous scaffolds has attracted increasing attention to satisfy requirements in the biomedical field. The advanced manufacturing technique of 3D printing can accurately control the geometry of the scaffold materials. Herein, the prepared HIPEs containing a PCL concentration of ≥ 4 w/v% could be used as 3D printing ink because of their gel-like nature and significant shear thinning

behaviour. For 3D printing, the HIPEs were placed into a polypropylene syringe and then pneumatically extrusion printed to form the designed emulsion scaffolds of different geometry (Figure 8 and Figure S16). The printed emulsion scaffolds possessed interconnected regular mm-scale macropores. Moreover, the printed porous scaffolds once dry were easily obtained by *in situ* cross-linking of the printed scaffolds followed by freeze drying. In order to view the inner structure, the cross-section of filament for a 3D printed porous scaffold with square shape was imaged using SEM. As seen from Figure S17, the printed filament had interconnected micropores internally, which indicated that the typical interconnected micropore structure of HIPE-based porous scaffolds is maintained after 3D printing. Thus, the gel-like HIPEs could be printed to prepare personalized porous scaffolds with various geometry and multistage pore structure (mm scale macropores resulting from 3D printing and μm micropores coming from HIPE template).

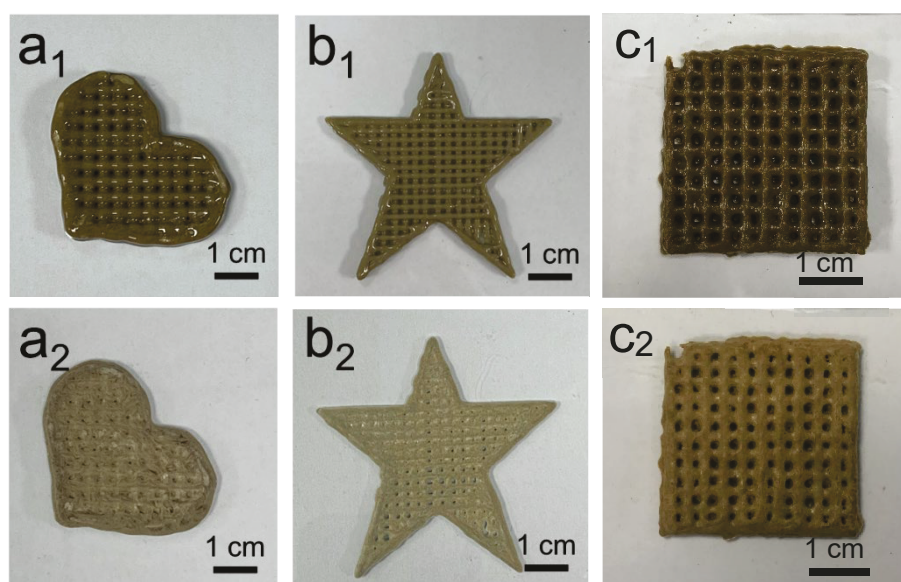


Figure 8. Digital photos of (upper) emulsion scaffolds and (lower) printed dry porous scaffolds of different shape based on 3D printing of HIPEs containing 4 w/v% PCL.

CONCLUSIONS

We have developed a facile and effective approach to construct PCL-embedded lignin-chitosan porous scaffolds based on the one-pot method of templating O/W Pickering HIPEs. The nanocomposite porous scaffolds displayed interconnected and well-defined pore structures with the PCL polymer layer embedded on the inner walls, with the scaffold porosity reaching more than 92%. Compression tests revealed that the introduction of hydrophobic PCL into the lignin-chitosan scaffold matrix was beneficial to the mechanical performance of the scaffolds. The absorption ratio by water of the porous scaffolds greatly reduced upon increasing the PCL concentration, enabling the scaffolds to retain their integrity in aqueous environments. Moreover, *in vitro* release of the antibacterial drug ENR displayed a slow drug release profile which decreased at higher PCL concentrations. Additionally, *in vitro* antibacterial assays confirmed that the porous scaffolds without ENR possessed antimicrobial activity against *E. coli* and *S. aureus*, and loading of ENR into the scaffold matrix significantly improved the antimicrobial activity. Finally, combining Pickering HIPEs with 3D printing technology can be used to construct porous biomass-based scaffold materials with personalized structure and geometry.

ASSOCIATED CONTENT

Supporting Information

This information is available free of charge *via* the internet at <http://pubs.acs.org/>.

Purification of lignin. Chemical structures of chitosan and genipin. Zeta potential of

lignin nanoparticles and complex nanoparticles. **TEM image and** size distribution of complex nanoparticles. Photos of drop test of Pickering HIPE dispersed in water and dichloromethane. Photos of emulsions taken immediately after preparation in different systems. **CLSM image of Pickering HIPE.** Droplet size distributions and mean diameters of Pickering HIPEs prepared with different PCL concentrations. Mechanism of the cross-linking reaction between chitosan and genipin. Pore size distributions and mean size of porous scaffolds prepared with different PCL concentrations. Compressive stress-strain curves of the composite porous scaffolds with different PCL concentrations without cross-linking by genipin. TGA curves of porous scaffolds prepared with different PCL concentrations. FTIR spectra of ENR and composite porous scaffolds without ENR and with ENR. **Photo of the 3D print procedure for preparing emulsion scaffold.** SEM image of the inner structure of filament for 3D printed scaffold.

AUTHOR INFORMATION

Corresponding Authors

*E-mail address: huyang0303@scau.edu.cn (Y. Hu); b.p.binks@hull.ac.uk (B.P. Binks); yangzhuohong@scau.edu.cn (Z. Yang).

ORCID

Yang Hu: 0000-0001-6856-9760; Bernard P. Binks: 0000-0003-3639-8041;

Zhuohong Yang: 0000-0002-7431-1501.

Author Contributions

Yaozong Li: Conceptualization, Methodology, Investigation, Writing original draft.
Yingying Peng, Jian Liu, Teng Yuan: Data curation, Methodology, Resources, Visualization. **Wuyi Zhou, Xianming Dong, Chaoyang Wang:** Resources, Validation, Writing-review & editing. **Bernard P. Binks:** Data analysis, Writing-review & editing.
Yang Hu, Zhuohong Yang: Funding acquisition, Supervision, Project administration, Writing-review & editing. **Yaozong Li and Yingying Peng contributed equally to this work.**

Notes

The authors declare no competing financial interest.

ACKNOWLEDGMENTS

This work was financially supported by the Science & Technology Program of Guangdong Province (2022A0505050062, 2020A0505100051), the General Project of Department of Natural Resources of Guangdong Province (GDNRC[2021]47), the Science and Technology Innovation Fund Project on Forestry of the Guangdong Province (2017KJCX006), the National Natural Science Foundation of China (51703067), the Opening Project of Key Laboratory of Polymer Processing Engineering (South China University of Technology), Ministry of Education (KFKT2101) and the Foundation of Key Laboratory of Tropical Crop Products Processing of Ministry of Agriculture and Rural Affairs, P. R. China (KFKT201903, KFKT201904).

REFERENCES

- [1] Garot, C.; Bettega, G.; Picart, C. Additive manufacturing of material scaffolds for bone regeneration: toward application in the clinics. *Adv. Funct. Mater.* **2021**, *31*, 2006967.
- [2] Heras, K. L.; Santos-Vizcaino, E.; Garrido, T.; Gutierrez, F. B.; Aguirre, J. J.; Caba, K. P.; Guerrero, M. I.; Hernandez, R. M. Soy protein and chitin sponge-like scaffolds: From natural by-products to cell delivery systems for biomedical applications. *Green Chem.* **2020**, *22*, 3445-3460.
- [3] Wang, X.; Rivera-Bolanos, N.; Jiang, B.; Ameer, G. A. Advanced functional biomaterials for stem cell delivery in regenerative engineering and medicine. *Adv. Funct. Mater.* **2019**, *29*, 1809009.
- [4] Wang, S. J.; Jiang, D.; Zhang, Z. Z.; Chen, Y. R.; Yang, Z. D.; Zhang, J. Y.; Shi, J.; Wang, X.; Yu, J. K. Biomimetic Nanosilica-Collagen Scaffolds for In Situ Bone Regeneration: Toward a Cell-Free, One-Step Surgery. *Adv. Mater.* **2019**, *31*, 1904341.
- [5] Ahmed, S.; Ali, A.; Sheikh, J. A review on chitosan centred scaffolds and their applications in tissue engineering. *Int. J. Biol. Macromol.* **2018**, *116*, 849-862.
- [6] Ambekar, R. S.; Kandasubramanian, B. Progress in the advancement of porous biopolymer scaffold: tissue engineering application. *Ind. Eng. Chem. Res.* **2019**, *58*, 6163-6194.
- [7] Stoppel, W. L.; Ghezzi, C. E.; McNamara, S. L.; Black, L. D.; Kaplan, D. L. Clinical applications of naturally derived biopolymer-based scaffolds for regenerative medicine. *Ann. Biomed. Eng.* **2015**, *43*, 657-680.
- [8] Curvello, R.; Raghuwanshi, V. S.; Garnier, G. Engineering nanocellulose hydrogels

- for biomedical applications. *Adv. Colloid Interface Sci.* **2019**, 267, 47-61.
- [9] Olmos-Juste, R.; Alonso-Lerma, B.; Pérez-Jiménez, R.; Gabilondo, N.; Eceiza, A. 3D printed alginate-cellulose nanofibers based patches for local curcumin administration. *Carbohydr. Polym.* **2021**, 264, 118026.
- [10] Qi, X.; Su, T.; Zhang, M.; Tong, X.; Pan, W.; Zeng, Q.; Zhou, Z.; Shen, L.; He, X.; Shen, J. Macroporous hydrogel scaffolds with tunable physicochemical properties for tissue engineering constructed using renewable polysaccharides. *ACS Appl. Mater. Interfaces* **2020**, 12, 13256-13264.
- [11] Davoodi, S.; Davachi, S. M.; Golkhaje, A. G.; Shekarabi, A. S.; Abbaspourrad, A. Development and characterization of salvia macrosiphon/chitosan edible films. *ACS Sustain. Chem. Eng.* **2020**, 8, 1487-1496.
- [12] Joseph, S. M.; Krishnamoorthy, S.; Paranthaman, R.; Moses, J.; Anandharamakrishnan, C. A review on source-specific chemistry, functionality, and applications of chitin and chitosan. *Carbohydr. Polym. Technol. Appl.* **2021**, 2, 100036.
- [13] Rajabi, M.; McConnell, M.; Cabral, J.; Ali, M. A. Chitosan hydrogels in 3D printing for biomedical applications. *Carbohydr. Polym.* **2021**, 260, 117768.
- [14] Peng, Y.; Huang, H.; Wu, Y.; Jia, S.; Wang, F.; Ma, J.; Liao, Y.; Mao, H. Plant tannin modified chitosan microfibers for efficient adsorptive removal of Pb²⁺ at low concentration. *Ind. Crop. Prod.* **2021**, 168, 113608.
- [15] Zhang, E.; Li, W.; Gao, Y.; Lei, C.; Huang, H.; Yang, J.; Zhang, H.; Li, D. High-capacity reusable chitosan absorbent with a hydrogel-coated/aerogel-core structure and superhydrophilicity under oil for water removal from oil. *ACS Appl. Bio Mater.* **2020**,

3, 5872-5879.

[16] Liu, F.; Li, W.; Liu, H.; Yuan, T.; Yang, Y.; Zhou, W.; Hu, Y.; Yang, Z. Preparation of 3D printed chitosan/polyvinyl alcohol double network hydrogel scaffolds. *Macromol. Biosci.* **2021**, 21, 2000398.

[17] Yang, J.; Shen, M.; Luo, Y.; Wu, T.; Chen, X.; Wang, Y.; Xie, J. Advanced applications of chitosan-based hydrogels: From biosensors to intelligent food packaging system, A review. *Trends Food Sci. Technol.* **2021**, 110, 822-832.

[18] Liu, J.; Song, F. X.; Chen R. Y.; Deng, G. T.; Chao, Y. X.; Yang, Z. H.; Wu, H.; Bai, M.; Zhang, P.; Hu, Y. Effect of cellulose nanocrystal-stabilized cinnamon essential oil Pickering emulsions on structure and properties of chitosan composite films. *Carbohydr. Polym.* **2022**, 275, 118704.

[19] Rezaei, F. S.; Khorshidian, A.; Beram, F. M.; Derakhshani, A.; Esmaeili, J.; Barati, A. 3D printed chitosan/polycaprolactone scaffold for lung tissue engineering: hope to be useful for COVID-19 studies. *RSC Adv.* **2021**, 11, 19508-19520.

[20] Yang, W.; Fortunati, E.; Bertoglio, F.; Owczarek, J.; Bruni, G.; Kozanecki, M.; Kenny, J.; Torre, L.; Visai, L.; Puglia, D. Polyvinyl alcohol/chitosan hydrogels with enhanced antioxidant and antibacterial properties induced by lignin nanoparticles. *Carbohydr. Polym.* **2018**, 181, 275-284.

[21] Bertolo, M. R.; Paiva, L. B. B.; Nascimento, V. M.; Gandin, C. A.; Neto, M. O.; Driemeier, C. E.; Rabelo, S. C. Lignins from sugarcane bagasse: Renewable source of nanoparticles as Pickering emulsions stabilizers for bioactive compounds encapsulation. *Ind. Crop. Prod.* **2019**, 140, 111591.

- [22] Park, I. K.; Sun, H.; Kim, S. H.; Kim, Y.; Kim, G. E.; Lee, Y.; Kim, T.; Choi, H. R.; Suhr, J.; Nam, J. D. Solvent-free bulk polymerization of lignin-polycaprolactone (PCL) copolymer and its thermoplastic characteristics. *Sci. Rep.* **2019**, *9*, 1-11.
- [23] Jiang, B.; Chen, C.; Liang, Z.; He, S.; Kuang, Y.; Song, J.; Mi, R.; Chen, G.; Jiao, M.; Hu, L. Lignin as a wood-inspired binder enabled strong, water stable, and biodegradable paper for plastic replacement. *Adv. Funct. Mater.* **2020**, *30*, 1906307.
- [24] Kazzaz, A. E.; Fatehi, P. Technical lignin and its potential modification routes: A mini-review. *Ind. Crop. Prod.* **2020**, *154*, 112732.
- [25] Yang, W.; Owczarek, J.; Fortunati, E.; Kozanecki, M.; Mazzaglia, A.; Balestra, G.; Kenny, J.; Torre, L.; Puglia, D. Antioxidant and antibacterial lignin nanoparticles in polyvinyl alcohol/chitosan films for active packaging. *Ind. Crop. Prod.* **2016**, *94*, 800-811.
- [26] Zhang, X.; Morits, M.; Jonkergouw, C.; Ora, A.; Valle-Delgado, J. J.; Farooq, M.; Ajdary, R.; Huan, S.; Linder, M.; Rojas, O. Three-dimensional printed cell culture model based on spherical colloidal lignin particles and cellulose nanofibril-alginate hydrogel. *Biomacromolecules* **2020**, *21*, 1875-1885.
- [27] Culebras, M.; Barrett, A.; Pishnamazi, M.; Walker, G. M.; Collins, M. N. Wood-derived hydrogels as a platform for drug-release systems. *ACS Sustain. Chem. Eng.* **2021**, *9*, 2515-2522.
- [28] Gazzurelli, C.; Migliori, A.; Mazzeo, P. P.; Carcelli, M.; Pietarinen, S.; Leonardi, G.; Pandolfi, A.; Rogolino, D.; Pelagatti, P. Making agriculture more sustainable: an environmentally friendly approach to the synthesis of lignin@Cu pesticides. *ACS*

Sustain. Chem. Eng. **2020**, 8, 14886-14895.

[29] Zhang, Y.; Liao, J.; Fang, X.; Bai, F.; Qiao, K.; Wang, L. Renewable high-performance polyurethane bioplastics derived from lignin-poly (ϵ -caprolactone). *ACS Sustain. Chem. Eng.* **2017**, 5, 4276-4284.

[30] Chen, K.; Qian, Y.; Wang, C.; Yang, D.; Qiu, X.; Binks, B. P. Tumor microenvironment-responsive, high internal phase Pickering emulsions stabilized by lignin/chitosan oligosaccharide particles for synergistic cancer therapy. *J. Colloid Interface Sci.* **2021**, 591, 352-362.

[31] Chen, K.; Qiu, X.; Yang, D.; Qian, Y. Amino acid-functionalized polyampholytes as natural broad-spectrum antimicrobial agents for high-efficient personal protection. *Green Chem.* **2020**, 22, 6357-6371.

[32] Wang, D.; Jang, J.; Kim, K.; Kim, J.; Park, C. B. "Tree to bone": lignin/polycaprolactone nanofibers for hydroxyapatite biomineralization. *Biomacromolecules* **2019**, 20, 2684-2693.

[33] Tang, C. M.; Chai, Y. Y.; Wang, C. X.; Wang, Z. X.; Min, J. W.; Wang, Y. F.; Qi, W.; Su, R. X.; He, Z. M. Pickering emulsions stabilized by lignin/chitosan nanoparticles for biphasic enzyme catalysis. *Langmuir* **2022**, 38, 12849-12858.

[34] Saz-Orozco, B. D.; Oliet, M.; Alonso, M.; Rojo, E.; Rodríguez, F. Formulation optimization of unreinforced and lignin nanoparticle-reinforced phenolic foams using an analysis of variance approach. *Compos. Sci. Technol.* **2012**, 72, 667-674.

[35] Chen, Y.; Zheng, K.; Niu, L.; Zhang, Y.; Liu, Y.; Wang, C.; Chu, F. Highly mechanical properties nanocomposite hydrogels with biorenewable lignin

- nanoparticles. *Int. J. Biol. Macromol.* **2019**, 128, 414-420.
- [36] Abasalta, M.; Asefnejad, A.; Khorasani, M. T.; Saadatabadi, A. R. Fabrication of carboxymethyl chitosan/poly (ϵ -caprolactone)/doxorubicin/nickel ferrite core-shell fibers for controlled release of doxorubicin against breast cancer. *Carbohydr. Polym.* **2021**, 257, 117631.
- [37] Hu, Y.; Wang, J.; Li, X.; Hu, X.; Zhou, W.; Dong, X.; Wang, C.; Yang, Z.; Binks, B. P. Facile preparation of bioactive nanoparticle/poly (ϵ -caprolactone) hierarchical porous scaffolds via 3D printing of high internal phase Pickering emulsions. *J. Colloid Interface Sci.* **2019**, 545, 104-115.
- [38] Voorde, K. M. V.; Pokorski, J. K.; Korley, L. T. Exploring Morphological Effects on the Mechanics of Blended Poly (lactic acid)/Poly (ϵ -caprolactone) Extruded Fibers Fabricated Using Multilayer Coextrusion. *Macromolecules* **2020**, 53, 5047-5055.
- [39] Abudula, T.; Gauthaman, K.; Mostafavi, A.; Alshahrie, A.; Salah, N.; Morganti, P.; Chianese, A.; Tamayol, A.; Memic, A. Sustainable drug release from polycaprolactone coated chitin-lignin gel fibrous scaffolds. *Sci. Rep.* **2020**, 10, 1-12.
- [40] Xu, Y. T.; Yang, T.; Liu, L. L.; Tang, C. H. One-step fabrication of multifunctional high internal phase Pickering emulsion gels solely stabilized by a softer globular protein nanoparticle: S-Ovalbumin. *J. Colloid Interface Sci.* **2020**, 580, 515-527.
- [41] Qiao, M.; Yang, X. C.; Zhu, Y.; Guerin, G.; Zhang, S. M. Ultralight aerogels with hierarchical porous structures prepared from cellulose nanocrystal stabilized Pickering high internal phase emulsions. *Langmuir* **2020**, 36, 6421-6428.
- [42] Hu, Y.; Gu, X.; Yang, Y.; Huang, J.; Hu, M.; Chen, W.; Tong, Z.; Wang, C. Facile

fabrication of poly (l-lactic acid)-grafted hydroxyapatite/poly (lactic-co-glycolic acid) scaffolds by Pickering high internal phase emulsion templates. *ACS Appl. Mater. Interfaces* **2014**, 6, 17166-17175.

[43] Wang, J.; Gao, H.; Hu, Y.; Zhang, N.; Zhou, W.; Wang, C.; Binks, B. P.; Yang, Z. 3D printing of Pickering emulsion inks to construct poly (D, L-lactide-co-trimethylene carbonate)-based porous bioactive scaffolds with shape memory effect. *J. Mater. Sci.* **2021**, 56, 731-745.

[44] Wei, Z. J.; Yang, Y.; Yang, R.; Wang, C. Y. Alkaline lignin extracted from furfural residues for pH-responsive Pickering emulsions and their recyclable polymerization. *Green Chem.* **2012**, 14, 3230-3236.

[45] Zou, T.; Sipponen, M. H.; Österberg, M. Natural shape-retaining microcapsules with shells made of chitosan-coated colloidal lignin particles. *Front. Chem.* **2019**, 7, 370.

[46] Zhao, X. Y.; Yu, G. B.; Li, J. C.; Feng, Y. H.; Zhang, L.; Peng, Y.; Tang, Y. Y.; Wang, L. Z. Eco-friendly Pickering emulsion stabilized by silica nanoparticles dispersed with high-molecular-weight amphiphilic alginate derivatives. *ACS Sustainable Chem. Eng.* **2018**, 6, 4105-4114.

[47] Liu, H.; Wang, C. Y.; Zou, S. W.; Wei, Z. J.; Tong, Z. Simple, reversible emulsion system switched by pH on the basis of chitosan without any hydrophobic modification. *Langmuir* **2012**, 28, 11017-11024.

[48] Mi, F. L.; Sung, H. W.; Shyu, S. S. Synthesis and characterization of a novel chitosan-based network prepared using naturally occurring crosslinker. *J. Polym. Sci.*

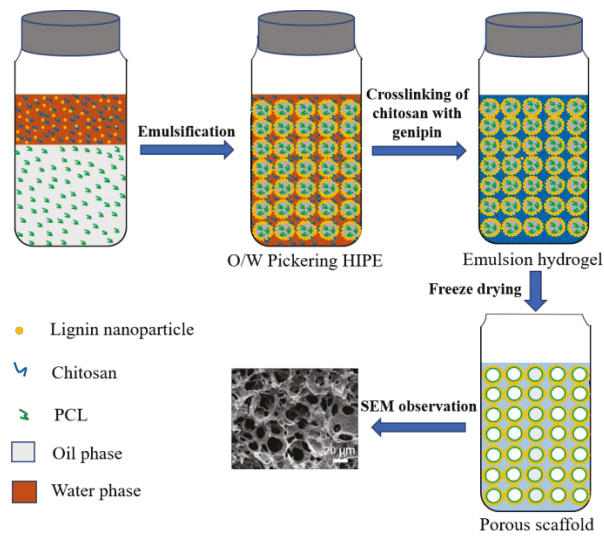
Part A: Polym. Chem. **2000**, 38, 2804-2814.

[49] Liu, F.; Li, W. Y.; Liu, H. T.; Yuan, T.; Yang, Y.; Zhou, W.; Hu, Y.; Yang, Z. H. Preparation of 3D printed chitosan/polyvinyl alcohol double network hydrogel scaffolds. *Macromol. Biosci.* **2021**, 21, e2000398.

[50] Butler, M. F.; Ng, Y. F.; Pudney, P. D. A. Mechanism and Kinetics of the Crosslinking Reaction between Biopolymers Containing Primary Amine Groups and Genipin. *J. Polym. Sci. Part A: Polym. Chem.* **2003**, 41, 3941-3953.

[51] Yu, Y. B.; Xu, S.; Li, S. M.; Pan, H. Genipin-cross-linked hydrogels based on biomaterials for drug delivery: a review. *Biomater. Sci.* **2021**, 9, 1583.

Table of Contents



A facile approach was developed to fabricate hydrophobic biopolymer-embedded biomass-based nanocomposite porous scaffolds by freeze drying based on O/W Pickering high internal phase emulsion templates.